Effect Of Nanofluids On The Performance Of Corrugated Channel Within Out-Of-Phase Arrangement

Dr Hassan Majdi, Azher M. Abed

ABSTRACT: Numerical investigations in the channel with lower and upper corrugated plate under constant heat flux conditions using nonafluids are carried out. CFD model by a finite volume method (FVM) with the structured uniform grid system is employed to solve the continuity, momentum and energy equations. The flow and heat transfer developments are simulated by using the k-ε standard turbulent model. The corrugated plates with corrugated tilt angle of 60° are tested with the height of the channel of 17.5 mm and wavy height of 2.5 mm. The model was simulated for the Reynolds number in the range of 5000 -20000. Studies are carried out for SiO_2 nanoparticles with different volume fractions in the range of 0%-4% and different nanoparticles diameters in the range of 20-80 nm. The results show that the heat transfer enhancement increased by using nonafluids as working fluid. The nanofluid with SiO_2 has the highest Nusselt number compared with base fluid . It is found that the average Nusselt number increased with the increase of volume fraction of the nanoparticles and Reynolds number, accompanied by a slight increase in pressure drop. It is found that with the decrease of nanoparticle diameter the Nusselt number increased for SiO_2 - water. Therefore, the nonafluids has a significant effect on the performance of heat transfer in the corrugated plate.

Keywords: Plate heat exchanger, Nanofluid, FVM, Nusselt number

1. INTRODUCTION

Increasing the demand for smaller and lightest high-performance devices drives for more efforts to optimize their heat and mass transfer characteristics. Traditional heat transfer fluids have inherently poor thermal conductivities. Many researchers have reported numerical and experimental studies on the thermal conductivity of nanofluids as presented below [1] measured the thermal conductivity of (EG) based nanofluid containing ZnO . To maximize the heat transfer efficiency with a smooth flow, the viscosity as well as the thermal conductivity should be considered as important physical properties of a nanofluid. [2-4] measured the thermal conductivity of nanofluids containing Al_2O_3 and CuO nanoparticles. Their results show that the thermal conductivity of the nanofluids increased with increasing volume fraction of the nanoparticles . [5, 6] investigated experimentally the relative effects of four types of nanofluids containing Al_2O_3 ,CuO, SiO_2 and ZnO dispersed in a base fluid of 60:40 (by mass) ethylene glycol and water mixture.

- *Dr Hassan Majdi, Azher M. Abed*
- *Department of Air conditioning and Refrigeration, Al-Mustaqbal University College*
- *Solar Energy Research Institute, Universiti Kebangsaan Malaysia (UKM), Locked Bag No: 320, 43600 Bangi, Selangor, Malaysia*
- *E-mail address: azher_muhson@yahoo.com*

Apart from various works on the corrugated channels to enhance heat transfer process,[7-13] Their results concluded that the use of nanofluids in plate heat exchanges can lead to size reductions of the overall system and more efficient use of the heat transfer fluids. The above survey; the numerous experimental and theoretical studies have been reported concerning the heat transfer enhancement using nanofluids in the CPHE. However, no data reported on thermal and flow field in the corrugated channel within out-of-phase arrangement using nanofluids. The objective of this paper is to numerical investigation in the corrugated channel with V- corrugated channel using different type of nanofluids.

2. Mathematical Modeling

2.1 Physical Model and Assumptions

The schematic diagram of the present problem is shown in Fig.1 which consisted of a two symmetric corrugated plate. The wall of the channel is composed of a flat wall and a corrugated wall. The length of each adiabatic flat section before, and after the corrugated section is 100 - 200 mm.

2.2 Governing Equations

By considering the geometry and physical problem as shown in Fig.1, the k-ε standard turbulence model [14, 15]is used to simulate the turbulent heat transfer and flow characteristics. The main governing equations [14, 15] can be written in the following form:

Continuity equation:

$$\frac{\partial \rho}{\partial t} + \mathrm{div}(\rho U) = 0 \qquad (2.1)$$

For an incompressible fluid (i.e. a liquid) the density ρ is constant and equation (3.1) becomes [16].

$$\mathrm{div}\, U = 0 \qquad (2.2)$$

Momentum equation:

$$\text{X-Momentum: } \rho\frac{Du}{Dt} = -\frac{\partial p}{\partial x} + \text{div}(\mu \text{ grad } u) + SM_X \quad (2.3)$$

$$\text{Y-Momentum: } \rho\frac{Dv}{Dt} = -\frac{\partial p}{\partial y} + \text{div}(\mu \text{ grad } v) + SM_y \quad (2.4)$$

Where P is the pressure (Pa), μ the viscosity (Pa s) and SM_X and SM_y the source term in the x and y direction.

Energy equation:

$$\rho\frac{Di}{Dt} = -p\text{div } U + \text{div}(\Gamma \text{ grad } T) + \phi + S_i \quad (2.5)$$

where

$$\mu_t = (\rho C_\mu k^2)/\varepsilon$$

$$C_\mu = 0.09 \ , C_{\varepsilon 1} = 1.47 \ , C_{\varepsilon 2} = 1.92 \ , \sigma_k = 1.0, \ \sigma_\varepsilon = 1.3$$

2.3 Methods of Calculation

In the present study, the solution of the governing equations of pressure drop, wall shear stress, friction factor, turbulence intensity ,average heat transfer rate, average Nusselt number , effective density , heat capacity and the effective thermal conductivity of the nanofluid .The methods of calculations for the mentioned terms, as [17], Defined and derived, are locally presented hereinafter, but together with our assumptions and simplifications: The average heat transfer coefficient along the corrugated channel h_c, can be calculated from the average heat transfer rate obtained from [18]:

$$Q_{ave} = h_c \, A_c \, (\Delta T) \quad (2.6)$$

where A_c is the surface area of the corrugated plate. The average heat transfer coefficient is presented in terms of average Nusselt number [18]as follows:

$$Nu = \frac{h_c \, H \, \tilde{\aleph}}{k \, Lc} \quad (2.7)$$

where H is the half distance of the channel height, k is the thermal conductivity of liquid ,Lc is the distance from the leading edge of the corrugated plate to the end of the domain , and $\tilde{\aleph}$ is the distance from the leading edge of the corrugated plate along the corrugated surface as shown in Fig.1. The local heat transfer h(x) is defined as :

$$h(x) = q \ / T_s(x) - T_b(x) \quad (2.8)$$

q represents the heat flux, $T_s(x)$ and $T_b(x)$ are the local surface wall and bulk temperatures, respectively. At the corrugated channel section, the inlet water temperature was taken as 300 K and the inlet water velocity was calculated using :

$$u_{in} = \frac{R_e \, \mu}{\rho D_h} \quad (2.9)$$

The hydraulic diameter is computed as [8]:

$$D_h = \frac{4A}{P} = H_{min} + H_{max} \quad (2.10)$$

Where Hmin and Hmax are the height of the lower and the upper corrugated channel as shown in Fig.1. The friction factor is defined as [19]:

$$f = 4C_{fx} \quad (2.12)$$

The Fanning friction factor is defined as follows:

$$C_{fx} = 2 \ \tau_s / \rho \ u_{in}^2 \quad (2.13)$$

τ_s is wall shear stress. The pressure drop for the flow in the corrugated channel is computed as [19]:

$$\Delta p = f\frac{Lc \ \rho u_{in}^2}{2D_h} \quad (2.14)$$

Turbulence intensity is the ratio of the root mean square of the turbulent velocity fluctuation at a particular location of the average of the velocity at the same location. It can be expressed as follows:

$$I = \frac{u'}{u} \times 100\% \quad (2.15)$$

where ,

u': The turbulence velocity

2.4 Properties of nanofluids

The effective density and heat capacity of the nanofluid at the reference temperature (T_0) is determined from the following equations [20]:

$$\rho_{nf} = (1-\phi)\rho_f + \phi\rho_p \quad (2.16)$$

Where ρ_f and ρ_{nf} are the mass densities of the based fluid and the solid nanoparticles, respectively.

$$(\rho \, C_p)_{nf} = (1-\phi)(\rho \, C_p)_f + \phi \, (\rho \, C_p)_p \quad (2.17)$$

Where $(\rho \, C_p)_f$ and $(\rho \, C_p)_p$ are heat capacities of the based fluid and the solid nanoparticles, respectively. By using Brownian motion of nanoparticles in corrugated channel, the effective thermal conductivity can be obtained by using the following mean empirical correlation [5, 6]:

$$k_{eff} = k_{static} + k_{Brwnian} \quad (2.18)$$

$$k_{static} = k_f \left[\frac{(k_p + 2k_f) - 2\phi \ (k_f - k_p)}{(k_p + 2k_f) + \phi \ (k_f - k_p)}\right] \quad (2.18.1)$$

$$k_{} \quad (2.18.2)$$

Where:

Boltzmann constant: =1.3807* 10^{-23} J/K

f((2.19)

Values of β for different particles are listed in Table 1 Modelling, f(T,ϕ), For 1% ≤ ϕ ≤ 4% and 300K<T<325K. The effective viscosity can be obtained by using the following mean empirical correlation [20]:

$$\mu_{eff} = \mu_f \frac{1}{(1-34.87\,(d_p/d_f)^{-0.3}*\phi^{1.03})}, d_f = \left[\frac{6M}{N\pi\rho_f}\right]^{1/3}$$

M: is the molecular weight of base fluid., N: is the Avogadro number = 6.022*1023 mol-1, ρ_f: is the mass density of the based fluid calculated at temperature To=293K

2.5 Boundary Conditions

In this study, no slip and constant heat flux boundary conditions are applied on the test section as follows:

At the wall

$$u=0\ ,\ v=0\ ,\ q=q_{wall} \qquad (2.21)$$

where, u and v are the velocities.

Initial conditions:

At the inlet, the uniform profiles for all the properties are as follows:

$$u=u_{in}\ ,\ v=0\ ,\ T=T_{in}\ ,\ k=k_{in}\ ,\varepsilon=\varepsilon_{in} \qquad (2.22)$$

At the outlet, the flow may safely be assumed as fully developed, which implies negligible stream wise gradients of all variables.

$$\frac{\partial \emptyset}{\partial n}=0\ ;\ \emptyset=u, v, p, k, \varepsilon, \omega \qquad (2.23)$$

2.6 Numerical Computation

In order to simulate and compute the detailed fluid flow characteristics of the corrugated channel problem, a commercial CFD code, namely GAMBIT 2.0 and FLUENT 6.3 software package, were employed. The fluid flow governing equations is solved by using the finite volume method It is based on the control volume method, SIMPLEC algorithm of Versteeg and Malalasekera [15] is used to deal with the problem of velocity and pressure coupling. Second – order upwind scheme and structure uniform grid system are employed to discretize the main governing equation as shown in Fig.2. The solutions are considered to be converted when the normalized residual values reach (10^{-5}) for all variables.

2.7 Code Validations and Grid Testing

Fig.3 shows the average corrugated plate temperature for air flow through two opposite corrugated plats is calculated and compared with a numerical and experimental study of Naphon [18]. It is observed that the results are in good agreement. To achieve the goal of having a near-wall modeling approach that will possess the accuracy of the standard two-layer approach for fine near-wall meshes and that, at the same time, will not significantly reduce the accuracy for wall-function meshes, four different meshes were tested, to evaluate the number of elements required. To test the grid independence, the grid sizes 24000, 34000, 48000 and 88000. It is found that after 48000 cells, further increase in cells gives less than 2% variation in average Nusselt number value which is taken as a criterion for grid independence.

3. Results and Discussion

3.1 Effect of SiO_2 Nanoparticles

In this section, the type of nanoparticle which is, SiO_2 and and pure water as a base fluid are used. The Nusselt number for SiO_2 nanofluids at wavy angle =60°, wavy height =2.5 mm, channel height =17.5 mm and different Reynolds numbers are shown in Fig. 4. It is seen that the SiO_2 nonafluids possess a higher Nusselt number compared to pure water. This is due to that the fluid velocity plays significant role on heat transfer, as the fluids move through the channel and SiO_2 having the highest average velocity, due to lowest density than base fluid [21]. The effect of SiO_2 nanofluids on the pressure drop is shown in Fig.5. The nanoparticle concentration considered is 4% for different Reynolds numbers. It can be seen that the SiO_2 nanofluids has the highest pressure drop. This is due to that the lower mean velocity gives the lower velocity gradient among the fluids, which in turn reduces the wall shear stress. The reduced friction results in lower pressure difference required to move the fluid along the channels, which is indicated by the pressure drop values [21].

3.2 The Effect of Different Nanoparticles Volume Fractions

Fig.6 illustrates the effects of nanoparticle and volume fraction on Nusselt number. It demonstrates that adding a low volume fraction of nanoparticle (0.01-0.04) with particle diameter of 20 nm for SiO_2 to the base fluid leads to significant increase in Nusselt number. The higher mass concentrations of nanoparticles compared to the base fluid molecules have higher momentum, this momentum carry and transfer thermal energy more efficiently at greater distance within the base fluid before releasing the thermal energy in colder regions of the fluid [13]. It can be seen that the Nusselt number increases with increased value of volume fraction. As indicated in the Fig.7 the results show that the pressure drop of the SiO_2 – water increases with the increase of Reynolds number and nanoparticle concentration. With an increase in the particle volumetric concentration in the nanofluids the density and viscosity increase and hence they cause an increased pressure drop [6]. Fig.8 illustrates that the increasing volume fraction of nanoparticles, which is responsible for large heat transfer performance leads to higher pressure drop. It should be noted that the enhancement in heat transfer increases with the increase of volume fraction of nanoparticles at the same value of the Reynolds number. It can be seen that for the same value of the volume fraction the heat transfer enhancement decreases slightly as the Reynolds number increases. Fig.9 gives the streamlines and isotherms contours for nanofluid flow in a wavy channel at Hw =

2.5,θ = 60°, Re=16000 and d_p= 20 nm for different volume fraction. The streamlines show that there is such appreciable change in flow pattern for a particular Re with increase the volume fraction.

3.3 The Effect of Different Nanoparticles Diameters

The working fluid SiO_2 – water is used to study the effect of nanoparticles diameters on the Nusselt number. The range of nanoparticles diameter used is 20-70 nm, volume fraction of 4% with different Reynolds numbers. As illustrated in Fig.10, for SiO_2 – Water nanofluid, decreasing the particle diameter leads to a higher Nusselt number. This is due aggregation of nanoparticles and stronger Brownian motion at smaller nano-particles diameters, which leads to higher thermal conductivity of nanofluids [13]].Similar trends of enhancement in Nusselt number by decreasing the particle diameter was obtained from [22]. As indicated in the Fig.11, the results show that the pressure drop of the SiO_2 – water increases with the increase of Reynolds number. It can be seen that the pressure drop increases with the decrease of nanoparticle diameters. This is due to the decrement of viscosity as the practical diameter increased for the same volume fraction. This observation is consistent with that presented by Vajjha [6].

4. Conclusions

In this paper, heat transfer enhancement and pressure drop due to flow SiO_2 nanofluids flowing in a corrugated channel under constant heat flux boundary condition are studied numerically for a range of Reynolds number of 8000 - 20000, nanoparticle volume fraction varying from 0 to 0.04 and nanoparticles diameters varying from of 20-80 nm .The effects of nanoparticle types, nanoparticle concentration (ø), nanoparticles diameter (dp) and type of base fluid on the thermal and hydraulic behavior of CPHE were examined. The results indicate that the SiO_2 gives the highest Nusselt number and pressure drop, while the pure water gives the lowest Nusselt number and pressure drop. It is also shown that the Nusselt number and pressure drop increased by increasing the nanoparticle volume fractions. The study noted that the Nusselt number increased with decreasing the nanoparticle diameter. In the cases examined, the highest enhancement in heat transfer was found at Reynolds number of 8000, nanoparticle volume fraction of 4%, and nanoparticle diameter of 20nm with an enhancement of around 18 % over the base fluid.

5-.References

[1]. Lee, G.-J., et al., Thermal conductivity enhancement of ZnO nanofluid using a one-step physical method. Thermochimica Acta, 2012. 542: p. 24-27.

[2]. H. Xie, et al., Thermal Conductivity Enhancement of Suspensions Containing Nanosized Alumina Particles. International Journal of Applied Physics, 2002. 91: p. 4568–72.

[3]. X. Wang, X.Xu, and S.U.S. Choi, Thermal Conductivity of Nanoparticle–Fluid Mixture. International Journal of Thermo Physic Heat Transfer, 1999. 13: p. 474–80.

[4]. S.K.Das, et al., Temperature Dependence of Thermal Conductivity Enhancement for Nanofluids. ASME Journal of Heat Transfer, 2003. 125: p. 567–74.

[5]. Vajjha, R.S. and D.K. Das, Experimental determination of thermal conductivity of three nanofluids and development of new correlations. International Journal of Heat and Mass Transfer, 2009. 52(21-22): p. 4675-4682.

[6]. Vajjha, R.S., D.K. Das, and D.P. Kulkarni, Development of new correlations for convective heat transfer and friction factor in turbulent regime for nanofluids. International Journal of Heat and Mass Transfer, 2010. 53(21-22): p. 4607-4618.

[7]. Ahmed, M.A., N.H. Shuaib, and M.Z. Yusoff, Numerical investigations on the heat transfer enhancement in a wavy channel using nanofluid. International Journal of Heat and Mass Transfer, 2012. 55(21-22): p. 5891-5898.

[8]. Ahmed, M.A., et al., Numerical investigations of flow and heat transfer enhancement in a corrugated channel using nanofluid. International Communications in Heat and Mass Transfer, 2011. 38(10): p. 1368-1375.

[9]. Heidary, H. and M.J. Kermani, Effect of nano-particles on forced convection in sinusoidal-wall channel. International Communications in Heat and Mass Transfer, 2010. 37(10): p. 1520-1527.

[10]. Pandey, S.D. and V.K. Nema, Experimental analysis of heat transfer and friction factor of nanofluid as a coolant in a corrugated plate heat exchanger. Experimental Thermal and Fluid Science, 2012. 38: p. 248-256.

[11]. Pantzali, M.N., A.A. Mouza, and S.V. Paras, Investigating the efficacy of nanofluids as coolants in plate heat exchangers (PHE). Chemical Engineering Science, 2009. 64(14): p. 3290-3300.

[12]. Santra, A.K., S. Sen, and N. Chakraborty, Study of heat transfer due to laminar flow of copper–water nanofluid through two isothermally heated parallel plates. International Journal of Thermal Sciences, 2009. 48(2): p. 391-400.

[13]. Seyf, H.R. and M. Feizbakhshi, Computational analysis of nanofluid effects on convective heat transfer enhancement of micro-pin-fin heat sinks. International Journal of Thermal Sciences, 2012. 58: p. 168-179.

[14]. B.E. Launder and D.B.Spalding, The Numerical Computation of Turbulent Flows Vol. 3. 1974: Comp. Meth. Appl. Mech. Eng.

[15]. H.K.Versteeg , W.M., An Introduction to Computational Fluid Dynamics 1995. : Longman Group.

[16]. J.Koo and C. Kleinstreuer, Viscous Dissipation Effects in Microtubes and Microchannels. International Journal of Heat and Mass Transfer, 2004. 47: p. 3159-3169.

[17]. Mohammed, H.A., A.M. Abed, and M.A. Wahid, The effects of geometrical parameters of a corrugated channel with in out-of-phase arrangement. International Communications in Heat and Mass Transfer, 2013. 40: p. 47-57.

[18]. Naphon, P., Effect of corrugated plates in an in-phase arrangement on the heat transfer and flow developments. International Journal of Heat and Mass Transfer, 2008. 51(15-16): p. 3963-3971.

[19]. F.P, I. and D. P.Dewitt, Fundamentals of Heat and Mass Transfer Vol. 5th Editions, . 2002: John Wiley & Sons,Inc.

[20]. Corcione, M., Heat Transfer Features of Buoyancy-Driven Nanofluids Inside Rectangular Enclosures Differentially Heated at the Sidewalls International Journal of Thermal Sciences, 2010. 49: p. 1536-1546.

[21]. H.A.Mohammed, et al., Numerical Study of Heat Transfer Enhancement of Counter Nanofluids in Rectangular Microchannel Heat Exchanger Superlattices and Microstructures, 2011. 50: p. 215-233.

[22]. Seyf, H.R. and B. Nikaaein, Analysis of Brownian motion and particle size effects on the thermal behavior and cooling performance of microchannel heat sinks. International Journal of Thermal Sciences, 2012. 58: p. 36-44.

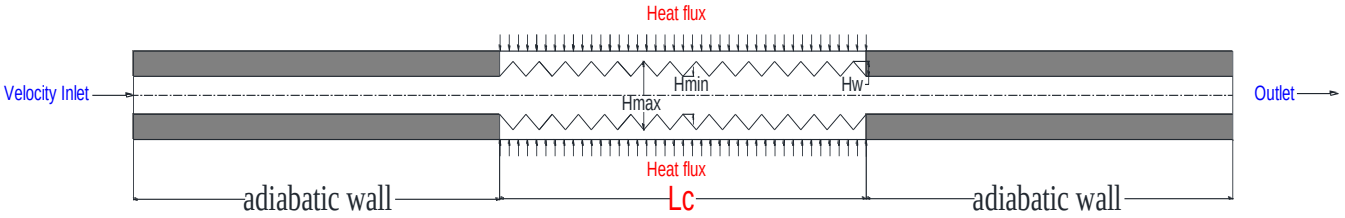

Fig. 1: Schematic Diagram of the Corrugated Channel.

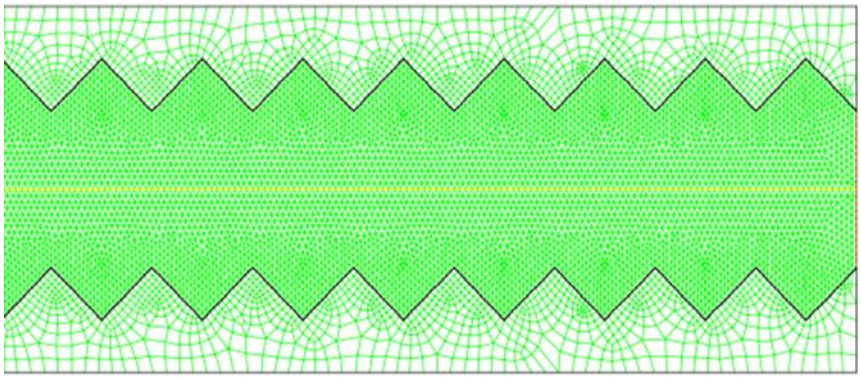

Fig.2: Schematic Diagram of the Structured Uniform Grid System

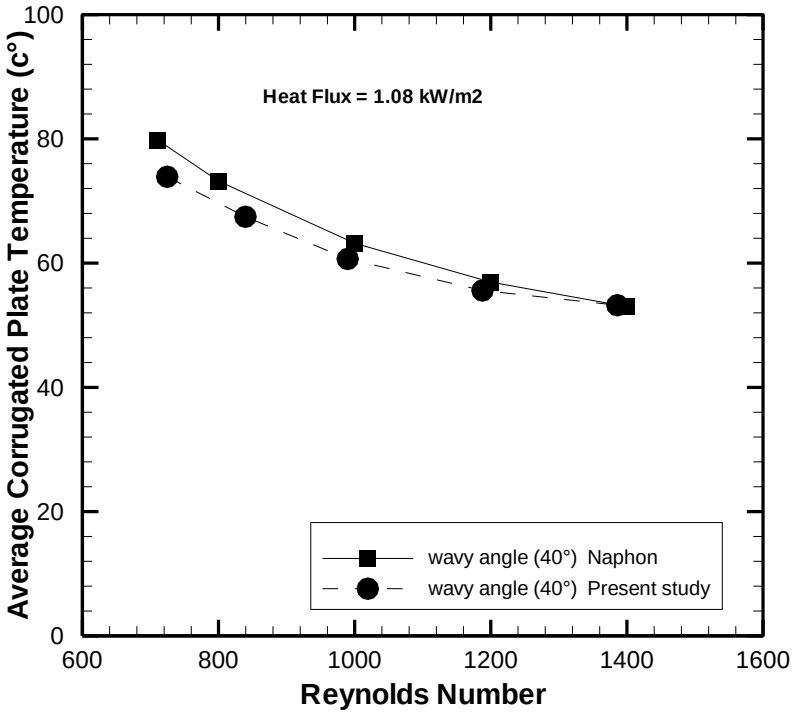

Fig.3: Comparison of the Average Corrugated Plate Temperature of the Present Study with the Results of Naphon [18] for Different Reynolds Numbers.

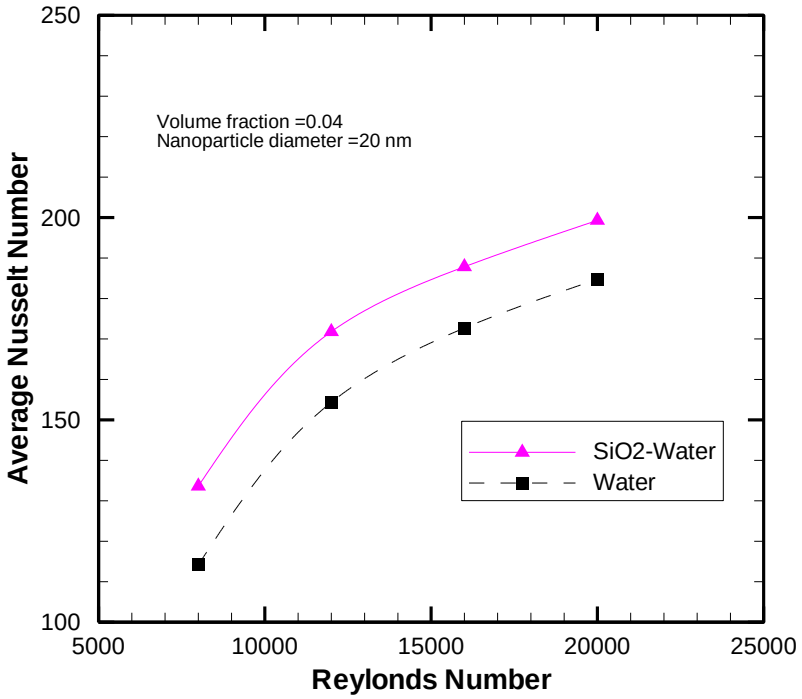

Fig.4: Nusselt Number for Channel with Different Nanofluids Types at Different Reynolds Number.

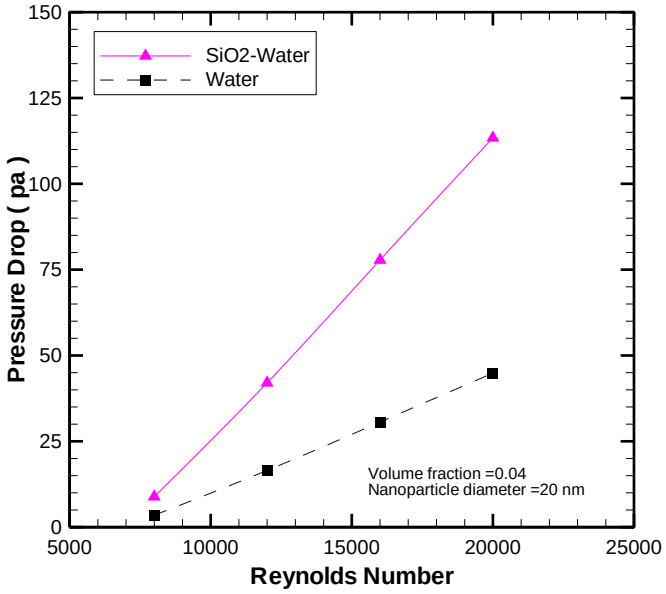

Fig. 5: Pressure Drop at Various Nanoparticles Types with Particle Volume Concentration of 4% for Different Reynolds Number.

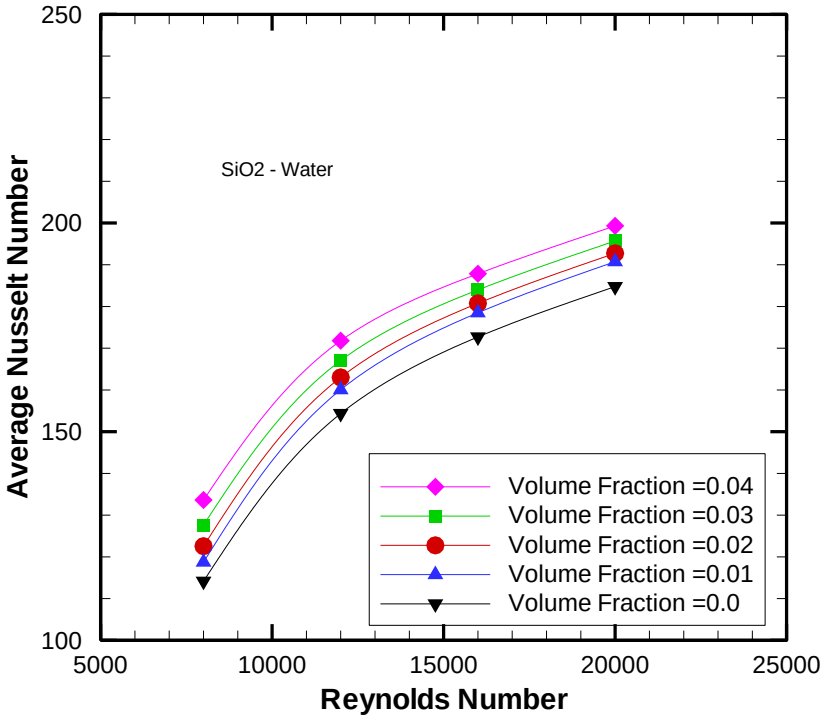

Fig. 6: Effect of Volume Fraction on the Nusselt Number at Various Reynolds Numbers.

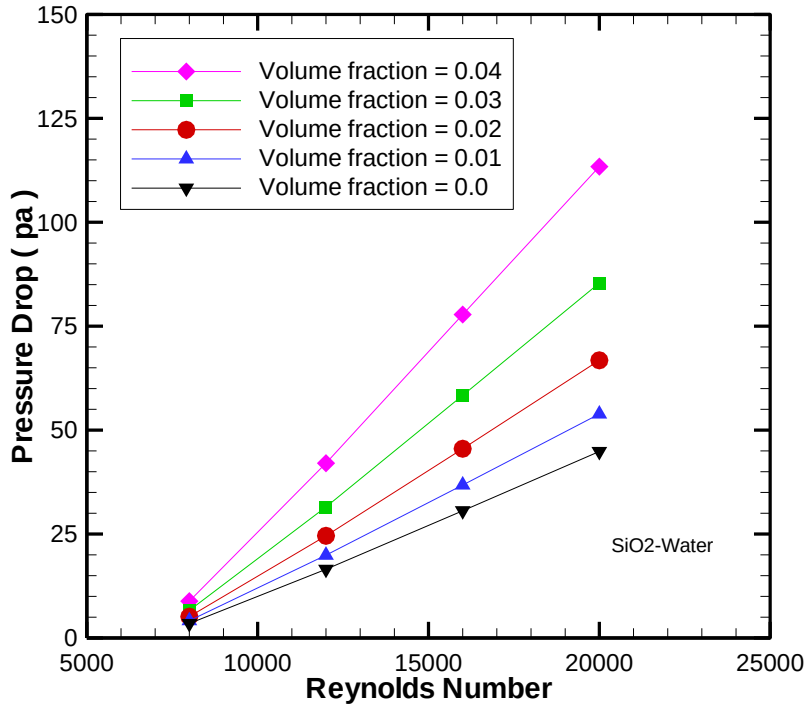

Fig.7: Pressure Drop of the SiO_2 Nanofluids at Various Particle Volume Concentrations as a Function of the Reynolds Number.

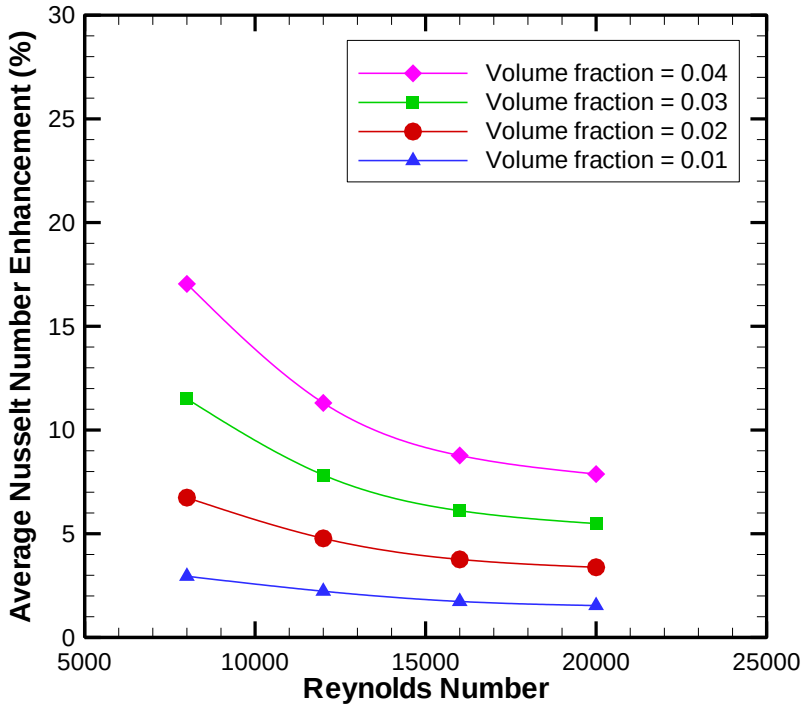

Fig .8: Average Nusselt Number Enhancement Versus Reynolds Number for Different Nanoparticle Concentrations

.

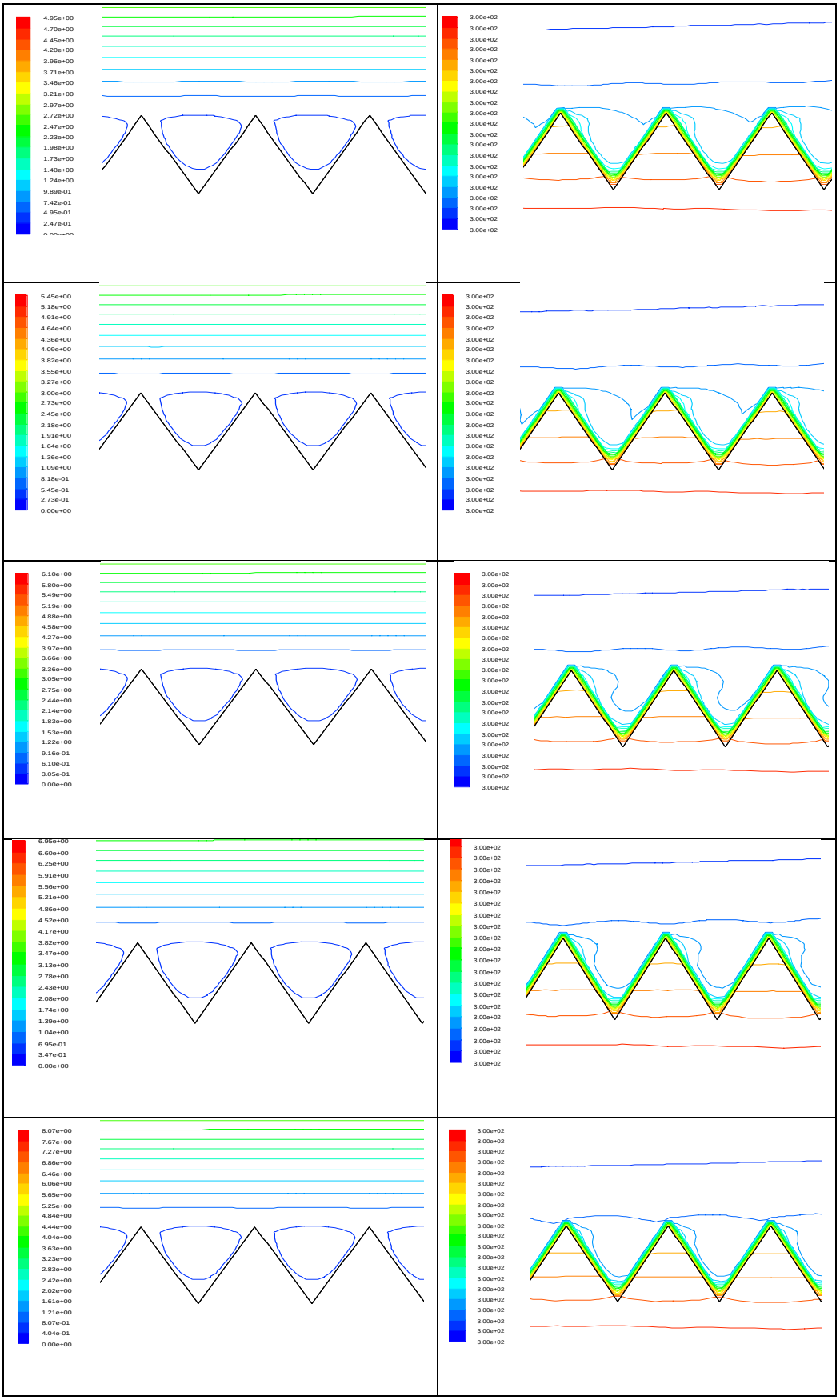

Fig.9: Streamlines (left) and Isotherms (right) Contours for Different Volume Fraction at, d_p=20 nm and Re=16000

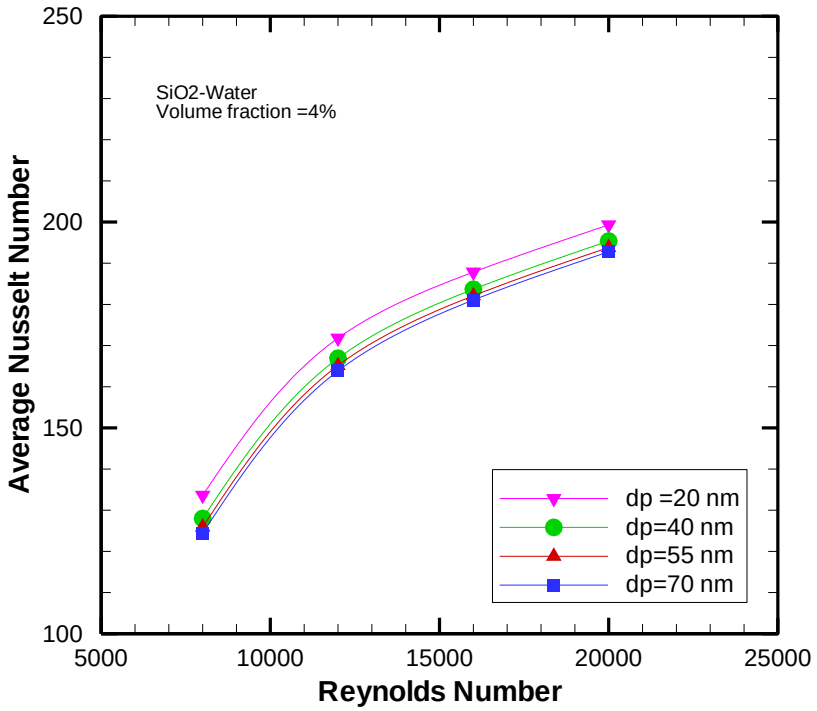

Fig.10: Average Nusselt Number Versus Reynolds Number of Different Nanoparticle Diameters.

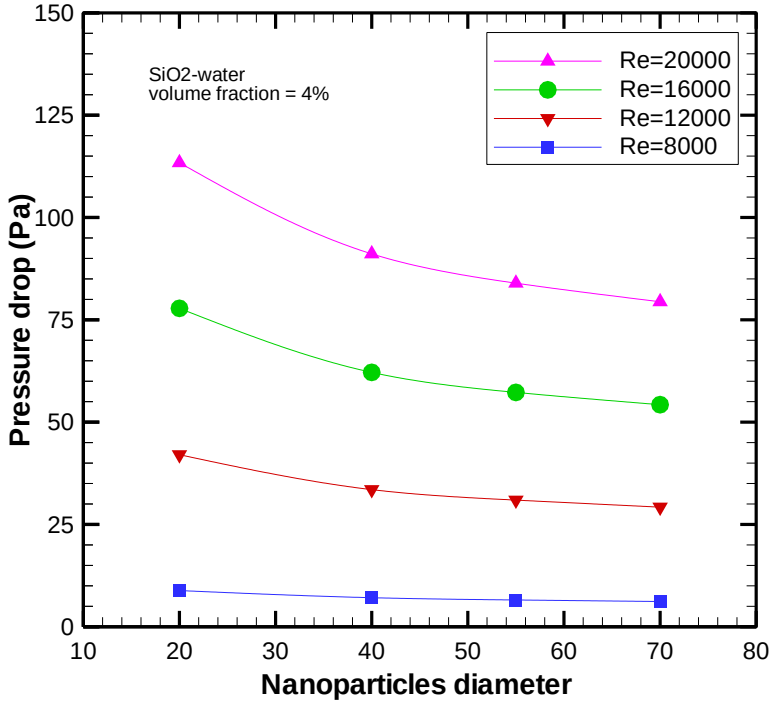

Fig.11: Pressure Drop Versus Different Nanoparticle Diameters of Different Reynolds Number.